error is dominated by the uncertainty of ϕ. Possible errors due to a systematic deviation from secular equilibrium and due to inaccuracies in the primary radium standard are not included.

4. ACKNOWLEDGMENTS

Energy Level Parameters from Nuclear Resonance Fluorescence at 7 Mev*†

K. REIBEL AND A. K. MANN
University of Pennsylvania, Philadelphia, Pennsylvania
(Received November 17, 1959)

The recoil-broadened photon spectrum from the reaction $F^{19}(p,\alpha\gamma)O^{16}$ has been used to measure the elastic photon scattering cross sections at 7 Mev of 31 elements. The observed angular distributions are consistent with dipole transitions. A plot of the cross sections versus mass number shows definite peaks around the closed shell regions near $Z=50$, $N=82$ (Sn, Te, and Ba), and $Z=82$, $N=126$ (Pb and Bi). For six medium and heavy elements self-absorption measurements were made which, when analyzed in terms of a number of nonoverlapping Breit-Wigner resonances, yield values of the average partial radiation widths to the ground states, the average total radiation widths, and the average level spacings for those elements. The radiation widths are significantly larger than those determined from slow-neutron scattering and capture experiments and, excepting Pb and Bi, the average level spacings are also appreciably greater than would be expected from the neutron data. The observed widths and spacings are in order of magnitude agreement with the recent interpretation of the modified single-particle calculation of Blatt and Weisskopf.

I. INTRODUCTION

MUCH of the presently available information on the radiation widths of highly excited nuclear energy levels (5 to 8 Mev above the ground state) of elements with $A \gtrsim 80$ has been obtained from neutron scattering and capture experiments from which it has been concluded that many of the measured properties of radiation widths are in general agreement with the statistical model of the compound nucleus.[1] First, the variation of the radiation widths, Γ_γ, with excitation energy and level spacing appears to support this conclusion and, in greater detail, to be consistent with the level density formula predicted by the statistical model. Second, the constancy of Γ_γ within a given nucleus and the variation of the average radiation width in passing from nucleus to nucleus indicate that de-excitation of the compound nucleus proceeds by gamma-ray emission to many lower levels, with the process in any given nucleus determined statistically. There remain, however, several problems of considerable interest relating to radiation widths. In particular, the absolute magnitude of the observed widths has received no satisfactory explanation. Under the assumption that the radiation is the result of motion of a single nucleon in the nucleus, Weisskopf[2] has derived expressions for the radiation widths for electric and magnetic radiation. For emission by highly excited states, Blatt and Weisskopf[3] have modified the single particle formulas to take into account the complexity of the emitting state. The ratio of the observed widths for magnetic and electric dipole emission appears to be in agreement with Weisskopf's formula, but the absolute values tend to be less than the predicted ones by about an order of magnitude.[1,4] Furthermore, the behavior of the radiation widths of nuclei in certain closed shell regions, where there is an appreciable reduction in level densities, is somewhat difficult to reconcile with a statistical description. Thus, Bi exhibits an average width similar to that of other heavy elements[1] and the spectra of the capture radiation of both Bi and Pb indicate that the intensities of the ground-state gamma rays are near 100%.[4,5]

[1] J. S. Levin and D. J. Hughes, Phys. Rev. **101**, 1328 (1956).

[2] V. S. Weisskopf, Phys. Rev. **83**, 1073 (1951).

[3] J. M. Blatt and V. F. Weisskopf, *Theoretical Nuclear Physics* (John Wiley & Sons, Inc., New York, 1952), Chap. XII.

[4] B. B. Kinsey and G. A. Bartholomew, Phys. Rev. **93**, 1260 (1954).

[5] B. P. Adyasevich, B. D. Groshev, and A. M. Demidov, *Conference of the Academy of Sciences of the U.S.S.R. on the Peaceful Uses of Atomic Energy, July* 1955 (Akademiia Nauk,

Resonance fluorescence, that is, the elastic scattering of photons, provides another effective method of investigating the radiation widths of nuclear energy levels. Its use has heretofore been confined largely to measurements in light elements where the excited states of interest are relatively widely spaced and are known to decay directly to the ground state.[6] Nevertheless, resonance fluorescence of gamma rays of an appropriate energy and spectral distribution might be expected to yield information on the radiation widths of heavy elements which is, at least, supplementary to that obtained in the neutron experiments. In particular, levels below the neutron binding energy and hence inaccessible by neutron capture can be excited. The criteria for the energy and spectral distribution of gamma rays for such measurements are reasonably well satisfied by the radiation from the reaction $F^{19}(p,\alpha\gamma)O^{16}$ which, for certain proton energies, is in the vicinity of 7 Mev and has a Doppler broadened spectrum of width about 130 kev. A fixed spectral distribution extended over this range of energy will encompass in the heavy elements a large number of levels and, consequently, the properties of individual levels cannot be determined by this method. If, however, the levels of concern in that interval are nonoverlapping, their average radiation width and spacing are directly related to measureable quantities; it is to this purpose that resonance fluorescence has been applied here. Finally, it is worth noting that this method involves the selective excitation of levels having large radiative transition matrix elements with the ground state, which fact, in conjunction with spin and parity selection rules, tends to limit the number of levels excited in any nucleus and hence to facilitate interpretation of the experimental results.

II. EXPERIMENTAL ARRANGEMENT

General

The experimental arrangement is shown schematically in Fig. 1. A horizontal beam of protons from the Brookhaven research Van de Graaff generator, after magnetic analysis, strikes a fluoride target and produces the reaction $F^{19}(p,\alpha\gamma)O^{16}$. The resulting photons, of energy about 7 Mev, with an energy spread of about 130 kev, scatter from a cylindrical scatterer into a NaI(Tl) detector which is shielded from a direct view of the source by a heavy metal cone. Pulses from the detector are amplified and analyzed in a 100-channel analyzer. The source intensity is continuously monitored with another scintillation counter. The angle of scattering is varied by changing the source-detector distance and, if necessary, also the scatterer radius. The scat-

terer is placed equidistant from source and detector so that runs with the detector at the scatterer position, when combined with the scattering and monitor data, permit direct evaluation of the absolute differential cross section for elastic scattering without knowledge of the absolute source intensity.

Photon Source

The Q value of the $F^{19}(p,\alpha\gamma)O^{16}$ reaction is $+8.124$ Mev. For a proton energy, E_p, less than about 2.5 Mev, the level in O^{16} at 8.87 Mev is the highest that can be excited.[7] This level is, however, very weakly excited and furthermore, only about 7% of the downward transitions go directly to the ground state, the remainder going to the levels at 6.14 Mev, (73%), 6.92 Mev, (5%), and 7.12 Mev, (15%).[8] In this experiment the proton energy was set at either 2.05 or 2.40 Mev and hence contributions to the gamma-ray flux are made only by transitions from the 6.14-, 6.92-, and 7.12-Mev levels to the ground state. Transitions from the 6.06-Mev level, with $J=0$, proceed by pair emission and may be neglected here.

The incident proton energy determines both the total photon yield and the relative intensities of the photons from the three levels mentioned above. Willard et al.[9] have investigated the total yield for E_p up to 5.4 Mev. The lower energy resonances had been studied previously by others.[10] Using a three crystal pair spectrometer,[11] we found the largest intensity ratio, $I(6.92+7.12)/I(6.14)$, at $E_p=2.05$ Mev,
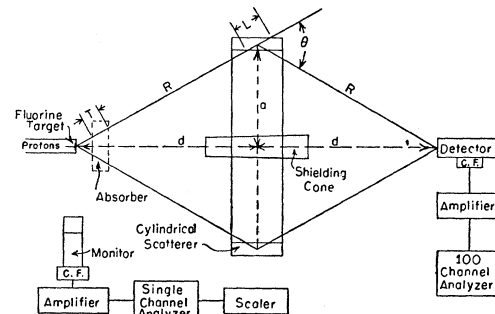

FIG. 1. Experimental arrangement exhibiting scattering geometry and block diagram of electronics. Shown are the scattering angle θ, the scatterer radius a, the photon source to detector distance $2d$, the path length in absorber T, the path length in scatterer L, and the photon source-scatterer and scatterer-detector distances R. The drawing is not to scale and, in particular, the monitor is over 10 feet away from photon source.

S.S.S.R., Moscow, 1955), session of the division of Physical Science [English translation by Consultants Bureau, New York: U. S. Atomic Energy Commission Report TR-2435, 1956 (unpublished)].

[6] F. R. Metzger, *Progress in Nuclear Physics*, Vol. 7 (Pergamon Press, London, 1959) p. 53.

[7] R. D. Bent and T. H. Kruse, Phys. Rev. **108**, 802 (1957).

[8] D. A. Bromley, *Proceedings of the Rehovoth Conference on Nuclear Structure* (North Holland Publishing Company, Amsterdam, 1958), p. 64.

[9] H. B. Willard, J. K. Bair, J. D. Kington, T. M. Hahn, C. W. Snyder, and F. P. Green, Phys. Rev. **85**, 849 (1952).

[10] C. Y. Chao, A. V. Tollestrup, W. A. Fowler, and C. C. Lauritsen, Phys. Rev. **79**, 108 (1950).

[11] See D. H. Wilkinson, B. J. Toppel, and D. E. Alburger, Phys. Rev. **101**, 673 (1956). We are grateful to Dr. Alburger for permission to use the three-crystal spectrometer for our measurements.

where the value is approximately 10. At this resonance the ratio $I(7.12)/I(6.92)$ also appears to be a maximum with a magnitude of approximately 4. This latter fact was determined by Swann and Metzger[12] by magnetic analysis of the α energies. It was further found that at $E_p = 2.40$ Mev this ratio is inverted, giving $I(7.12)/I(6.92)$ about $\frac{1}{4}$. At the higher proton energy, however, the ratio $I(6.92+7.12)/I(6.14)$ is reduced to about 4 because of the increased contribution from the 6.14-Mev level. In what follows, the unresolved 6.92- and 7.12-Mev radiation will be referred to as "7-Mev" radiation. It will be shown in the discussion of the detector properties that the contribution of the 6.14-Mev radiation to the measured scattering at 7 Mev is completely negligible at $E_p = 2.05$ Mev and is at most a few percent at $E_p = 2.40$ Mev.

Typical slowing-down times for a light nucleus such as O^{16} in a dense material are about 10^{-13} sec,[13] whereas the lifetimes of the 6.92- and 7.12-Mev levels are known to be approximately 10^{-14} sec.[12] The 7-Mev radiation is therefore emitted while the O^{16} nucleus is still recoiling from the preceding α emission, which gives rise to an appreciable Doppler broadening of the radiation. It can be shown that the resultant line shapes are rectangular if the O^{16} nuclei recoil isotropically in the center-of-mass system of the decaying Ne^{20}. Measurements of the photon yield as a function of angle were made for both $E_p = 2.05$ Mev and $E_p = 2.40$ Mev at $0°$, $15°$, $30°$, $45°$, and $60°$ (the last four values corresponding to scattering angles of $30°$, $60°$, $90°$, and $120°$, respectively, in the resonance fluorescence experiments discussed below). Within the experimental uncertainty, the assumption of isotropy of the O^{16} recoil appears justified. If an appreciable number of the recoiling O^{16} atoms had partially slowed down before emitting photons, this effect would round off the edges of a rectangular shape. Since, however, the mean lifetime of the 7-Mev levels is an order of magnitude less than the mean slowing-down time, and the velocity spectrum of the recoiling nuclei is unknown, it seems reasonable to assume a rectangular shape. The calculated energy spread of each of the spectral lines is then 127 kev at $E_p = 2.05$ Mev and 134 kev at $E_p = 2.40$ Mev.

To maximize the yield of 7-Mev radiation and still preserve known intensity ratios, it was necessary to utilize very high proton currents and relatively thin fluoride targets. In this experiment CaF_2 or SrF_2 was vacuum deposited on a gold backing over an area of about 1 cm in diameter to a thickness of about 1 mg/cm² (corresponding to an energy loss of approximately 100 kev for 2-Mev protons). The total yield of 7-Mev radiation from these targets at incident proton energies of 2.05 and 2.40 Mev was about 5×10^7 photons-sec⁻¹
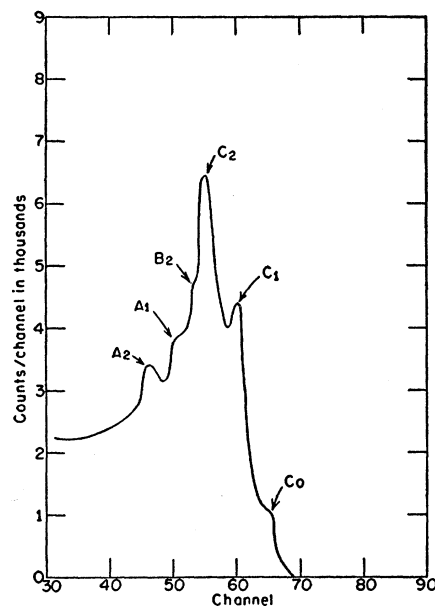
12 C. P. Swann and F. R. Metzger, Phys. Rev. 108, 982 (1957).
13 S. Devons, Proceedings of the Rehovoth Conference on Nuclear Structure (North Holland Publishing Company, Amsterdam, 1958), p. 547.


FIG. 2. Detector response at $E_p = 2.05$ Mev. The letters A, B, and C refer to 6.14-, 6.92-, and 7.12-Mev photons, respectively; the subscripts 0, 1, and 2 indicate, respectively, the full energy, one quantum escape, and two quantum escape peaks.

$-\mu a^{-1}$, and it was possible to run continuously for 20 hours at proton currents of 70 μa without noticeable decrease in the photon yield.

Scattering Geometry

The scattering geometry, aside from having a horizontal rather than vertical axis of symmetry, is quite similar to that used previously[14] and requires little discussion. With the scattering cylinder midway between the source and detector and its equatorial plane bisected perpendicularly by the line joining source and detector, it is possible to define a mean scattering angle as shown in Fig. 1 equal to 2 arctan (a/d), where a is the scatterer radius and $2d$ is the separation of source and detector. For a given a, it is necessary only to measure the linear distance $2d$ to set the angle of scattering. All scatterers were 10 cm wide which, together with the small size of the detector, permitted an angular resolution of ± 5 degrees.

Detector and Monitor

The gamma-ray detector consisted of a NaI(Tl) scintillator, $1\frac{1}{2}$ in. in diameter by 2 in. long and a 6292 photomultiplier tube. The scintillator was shielded by 1 cm of copper to reduce pileup of low-energy radiation. Signals from the detector passed through a cathode follower and a nonoverload linear amplifier into a 100-channel pulse-height analyzer with automatic print out.

14 A. M. Bernstein and A. K. Mann, Phys. Rev. 110, 805 (1958).
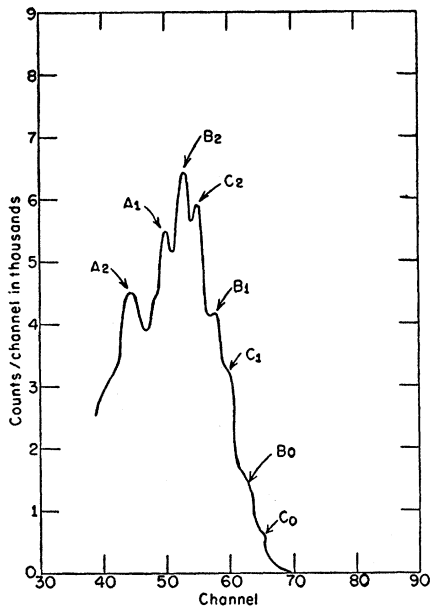
FIG. 3. Detector response at $E_p = 2.40$ Mev. The peaks are labeled according to the convention described in Fig. 2.

The relatively small size of the detector crystal had two advantages. As already stated, the spread in the angle subtended by the detector at the scatterer was kept small. In addition, the pulse-height spectrum of the elastically scattered radiation had a characteristic "signature" which permitted easy discrimination between the 6- and 7-Mev components. The detector response to the radiation produced by proton bombarding energies of 2.05 and 2.40 Mev is shown in Figs. 2 and 3, respectively. Figure 2 shows explicitly the preponderance of 7.12-Mev radiation and the negligible quantity of 6.14-Mev radiation above channel 52 at $E_p = 2.05$ Mev. In Fig. 3, the spectrum is more complex because of the dominance of the 6.92-Mev radiation, but the number of 6.14-Mev photons in the region above channel 52 is still less than 5% of the total.

The source monitor was also a NaI(Tl) scintillator $1\frac{1}{2}$ in. in diameter by 2 in. long mounted on a 6292 photomultiplier. It was located permanently to view the source from an appropriate distance. The differential pulse-height spectrum was examined regularly but during a scattering experiment only pulses above a given size from the monitor were counted.

Description of Measurements

A scattering experiment involved first a run with a scatterer in place for about 10^7 monitor counts, or roughly $\frac{1}{2}$ hour. Second, a run was made without the scatterer.[15] Finally, with the proton beam current considerably reduced, a run was made in which the shadow cone was removed and the detector placed in

[15] In the event a scatterer was enclosed in a container, the background run was made with the empty container in position.

the position previously occupied by the scatterer; because of the symmetry of the geometry, the detector efficiency and solid angle with respect to the 7-Mev radiation emanating directly from the source were the same as they had previously been with respect to the elastically scattered radiation from the scatterer. The last, or "direct" run utilized proton currents of about 0.05 μa for 10^8 monitor counts in about 5 minutes, and served to eliminate the need for separate, independent measurements of detector efficiency and solid angle. This procedure was repeated a number of times to obtain a value of the absolute differential cross section for elastic scattering by a given scattering material.

The pulse-height spectra of scattered radiation from bismuth, with a high cross section for elastic scattering, and from silver, with a low cross section, are shown in Figs. 4 and 5. The former spectrum clearly reproduces the features of the spectrum of the unscattered radiation (see Fig. 2) but these features are partially obscured in the data for silver. The value of the cross section is, however, determined from the area under the elastic region of the spectrum and is largely independent of the detailed structure of the pulse-height spectrum.

In self-absorption measurements a certain thickness of the material composing the scatterer is inserted between the source and the scatterer (Fig. 1) to filter out precisely those photons which give rise to resonant scattering. The experimental procedure was as described above, except that alternate sequences were made with and without absorber. To illustrate, with the absorber
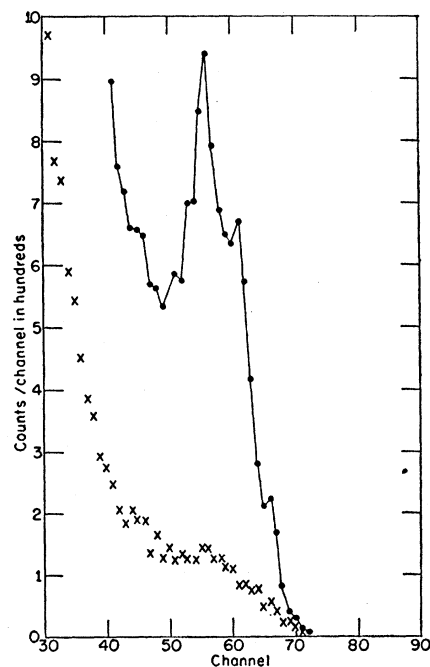

FIG. 4. Pulse-height spectrum of scattered radiation from an element with a large scattering cross section: Bi at 120°, $E_p = 2.05$ Mev, 4×10^6 monitor counts in 1910 sec. Crosses represent background measured with scatterer removed.

in the beam runs were made with the scatterer, without the scatterer, and with the detector in the scatterer position. Then, with the absorber removed, the same sequence was repeated.

Background

The main source of background at 7 Mev is radiation from neutron capture. Neutrons originate in the Van de Graaff, both from deuterium contamination of the beam and from (p,n) reactions. The contribution of capture radiation to the high-energy end of the observed pulse-height spectra for high elastic scattering cross-section elements may be estimated to be less than about 15% of the total rate by comparing the spectra of scattered and unscattered radiation. Further, the procedure of subtracting data obtained without a scatterer from that obtained with a scatterer should, to first approximation, eliminate the effect of neutron capture on the measured cross sections of all elements. Capture radiation arising from neutrons captured in a given scatterer or scattered into the detector by that scatterer will not be eliminated by this procedure, but the measured response of the detector to neutrons of energies in the range 1 to 2 Mev and consideration of neutron scattering and capture cross sections indicate that the uncertainty in our measured cross sections due to this background may be neglected in comparison with other experimental errors.
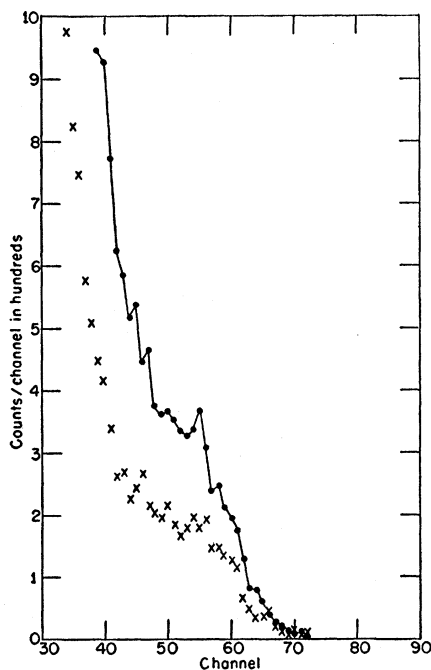

FIG. 5. Pulse-height spectrum of scattered radiation from an element with a small scattering cross section: Ag at 120°, $E_p = 2.05$ Mev, 7.5×10^6 monitor counts in 1680 sec. Crosses represent background measured with scatterer removed.
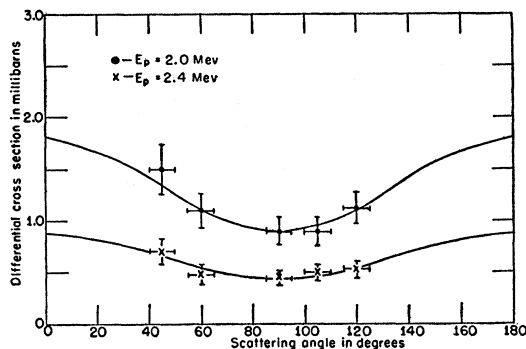

FIG. 6. Differential elastic cross sections of Pb. The curves $1 + \cos^2\theta$ are arbitrarily normalized at 90°, but within the experimental error the quality of the fit is independent of the normalization.

III. EXPERIMENTAL RESULTS

Elastic Scattering Cross Sections

The differential cross sections for elastic scattering at 90° of 31 naturally occurring elements were measured with $E_p = 2.05$ Mev. For 10 of the 31 elements, measurements were also made at 120° and, in most instances at 60°. These data are summarized in Table I. For natural lead, a more complete angular distribution was obtained which is shown in Fig. 6. All of the observed distributions are consistent with the form $a + b \cos^2\theta$, which holds for both electric and magnetic dipole transitions. Assuming only dipole transitions, total cross sections were calculated[16] for the 31 elements and are presented in Table II and Fig. 7. The elastic scattering cross sections for a few of the elements were so small that only upper limits could be assigned as indicated in Fig. 7. Upper limits were also assigned for samarium and gold because quantities of these elements sufficient to give count rates appreciably above the background were not available to us. The errors assigned to the

TABLE I. Differential cross sections for elastic scattering.

Proton energy Mev	Element	$\langle \bar{\sigma}(\theta) \rangle \times 10^{28}$ (cm²/sr)		
		60°	90°	120°
2.05	O	···	0.094±0.025	0.089±0.025
	Fe	···	0.24±0.04	0.42±0.06
	Cu	0.60±0.09	0.42±0.05	0.41±0.05
	Ag	0.73±0.10	0.47±0.07	0.48±0.10
	Sn	3.5±0.5	2.5±0.3	3.1±0.2
	Te	···	3.5±0.5	4.3±0.6
	Hg	···	2.1±0.2	2.4±0.3
	"Pb²⁰⁶"	8.2±1.0	6.3±0.5	···
	Pb	11±2	9.0±1.0	11±2
	Bi	12±2	13±1	11±2
	Th	0.53±0.08	0.51±0.08	0.32±0.05
2.40	O	···	0.19±0.05	0.097±0.025
	Cu	···	0.28±0.04	0.39±0.06
	Sn	···	2.7±0.4	3.0±0.5
	"Pb²⁰⁶"	6.1±0.9	5.9±0.9	···
	Pb	4.9±0.8	4.4±0.7	5.3±0.8

[16] See Sec. IV and Appendix B for the calculations.

TABLE II. Average total cross sections for elastic scattering.

Element	Spin[a]	$\langle\bar{\sigma}\rangle$ in mb $E_p=2.05$ Mev	$E_p=2.40$ Mev	Element	Spin[a]	$\langle\bar{\sigma}\rangle$ in mb $E_p=2.05$ Mev	$E_p=2.40$ Mev
B	$3/2^-$	<0.027	<0.27	Ag	$1/2^-$	0.65±0.10	
O	0^+	0.16±0.04	0.19±0.05	Cd	0^+	1.4±0.2	
F	$1/2^+$	<0.03		Sn	0^+	4.1±0.5	4.5±0.7
Al	$5/2^+$	<0.008		Sb	$5/2^+$	0.89±0.13	
Si	0^+	<0.057		Te	0^+	5.8±0.8	5.3±0.8
S	0^+	0.074±0.011		I	$5/2^+$	0.71±0.11	0.76±0.11
V	$7/2^-$	0.65±0.10		Ba	0^+	4.9±0.7	
Cr	0^+	0.30±0.05		Sm	0^+	<0.67	
Mn	$5/2^-$	0.31±0.05		W	0^+	1.8±0.4	
Fe	0^+	0.40±0.06		Au	$3/2^+$	<2.7	
Co	$7/2^-$	0.29±0.04		Hg	0^+	3.5±0.4	
Ni	0^+	0.20±0.02		Tl	$1/2^+$	3.9±0.6	2.1±0.3
Cu	$3/2^-$	0.57±0.06	0.38±0.06	"Pb^{206}"	0^+	10.5±0.8	9.9±1.5
Zn	0^+	0.86±0.13		Pb	0^+	15±2.2	7.4±1.2
Zr	0^+	1.0±0.1		Bi	$9/2^-$	17.5±1.3	12±2
Mo	0^+	1.4±0.2		Th	0^+	0.86±0.13	

[a] Ground-state spin and parity of dominant isotope or isotopes.

cross sections in Table II are the mean deviations obtained from several measurements on each of the scatterers.

A number of measurements were made at $E_p=2.40$ Mev. Within experimental error the form of the angular distributions remained the same as that at $E_p=2.05$ Mev, but the absolute values of the cross sections at the two energies were rather different for some elements. In particular, the total cross section of natural lead at $E_p=2.05$ Mev appears to be twice that at $E_p=2.40$ Mev which, using the values for $I(7.12)/I(6.92)$ given above, indicates that the total cross section at 7.12 Mev is almost four times the value at 6.92 Mev. The data at $E_p=2.40$ Mev are included in Tables I and II and the average cross sections at 6.92 and 7.12 Mev are presented in Table III.

Self-Absorption

Self-absorption measurements in the elastic region were made for six elements at $E_p=2.05$ Mev and the
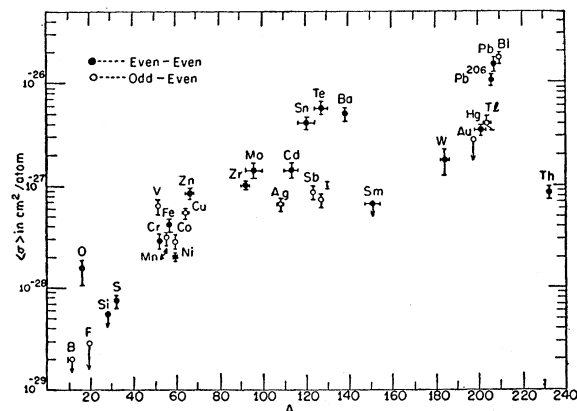

FIG. 7. Elastic scattering cross sections versus mass number. $E_p=2.05$ Mev. Horizontal lines indicate range in A of major isotopes in the natural elements used as scatterers. Not shown: upper limit for Al of 8.0×10^{-30} cm^2/atom.

results are shown in Table IV, which also includes data for Pb at $E_p=2.40$ Mev. The errors in the measured ratios are mean deviations. The magnitude of the effect of self-absorption in the raw data is illustrated in Fig. 8 which shows the pulse height spectra for a tin scatterer obtained without absorber, with absorber in the incident beam and with absorber but corrected for electronic absorption.[17] Absorption spectra obtained with the absorber placed in the scattered, rather than the incident beam, are shown in Fig. 9 which exhibits no self absorption presumably because the scattered radiation is no longer resonant.

It was of interest to cross absorb natural Pb with radiolead ("Pb^{206}"), and Bi with several absorbers. By cross absorption is meant an absorption experiment in which the absorber is of a different material than the scatterer. In the case of Pb and "Pb^{206}" there was some overlap of isotope content; Pb contains Pb^{204}, Pb^{206}, Pb^{207}, and Pb^{208} with relative abundances of 1%, 26%, 21%, and 52%, respectively, while the sample of "Pb^{206}" had Pb^{206}, Pb^{207}, and Pb^{208} in the amounts 88%, 9%, and 3%, respectively. The data indicate real

TABLE III. Average elastic scattering cross sections at 6.92 and 7.12 Mev.

Element	$\langle\bar{\sigma}_{7.1}\rangle$ mb	$\langle\bar{\sigma}_{6.9}\rangle$ mb	$\langle\bar{\sigma}_{7.1}\rangle/\langle\bar{\sigma}_{6.9}\rangle$
Cu	0.63±0.14	0.31±0.07	2.0±0.6
Sn	4.0±0.8	4.6±0.9	0.9±0.2
Te	6.0±1.2	5.2±1.0	1.1±0.3
I	0.69±0.15	0.77±0.17	0.9±0.3
Tl	4.4±1.0	1.6±0.4	2.8±0.9
"Pb^{206}"	11±1.6	9.7±1.5	1.1±0.3
Pb	18±4	4.8±1.1	3.7±1.1
Bi	19±4	10±2	1.9±0.6

[17] The explicit correction for electronic absorption in the absorber made in Figs. 8 and 9 is not necessary in treating the data to extract nuclear energy level parameters. For details see Sec. IV.

cross absorption of Pb with "Pb206" but, unfortunately, do not uniquely identify the isotopic combinations responsible for the large observed resonant scattering. Cross absorption of Pb and Sn absorbers with a Bi scatterer produced a null effect within experimental error, although Fuller and Hayward[18] have reported observing cross absorption for a Pb absorber and Bi scatterer. The difference in the two results may be due to the difference in the incident photon spectra of the two experiments; their bremsstrahlung spectrum extended from 4 to 7.5 Mev, or roughly 30 times the spectral range of this experiment.

Inelastic Scattering

Scattered radiation of energy less than that of the incident radiation, namely inelastic scattering, may arise from scattering by electrons or from the decay of an excited nucleus involving the emission of several photons. Measurement of the latter process is particularly desirable because it, in conjunction with elastic

TABLE IV. Results of self-absorption measurements.[a]

Element	Path length in absorber T (cm)	Path length in scatterer L (cm)	R[b]	$\bar{\Gamma}_{\gamma 0}/\bar{\Gamma}_\gamma$
Cu	3.58	1.79	0.64±0.08	0.15±0.1
Ag	3.58	0.89	0.70±0.12	0.06±0.04
Sn	2.95	0.89	0.72±0.11	0.2±0.1
Hg	3.13	1.41	0.66±0.11	0.07±0.03
"Pb206"	2.05	0.51	0.47±0.08	0.6±0.3
Pb	2.20	0.49	0.54±0.04	0.6±0.3
Pb[c]	2.05	0.51	0.73±0.11	0.2±0.1
Bi	2.61	0.61	0.71±0.09	0.3±0.2

a All measurements at E_p =2.05 Mev except as indicated.
b Ratio of counts in elastic region with and without absorber.
c E_p =2.40 Mev.

scattering data, determines directly the branching ratio of transitions from the excited nuclear levels.

At 7 Mev, the total electronic cross section of roughly 10 barns for the heavier elements is shared almost equally between Compton scattering and pair production but neither of these effects is expected to contribute appreciably to the scattered radiation of this experiment at energies above about 3 Mev. This was verified for Compton scattering by observing that at a scattering angle of 60°, where the Compton radiation had an energy of 1 Mev, the scattering from different elements did in fact exhibit a linear dependence on Z. At energies greater than about 4 Mev, however, the observed scattering showed an appreciable electronic contribution with a pronounced, approximately cubic, dependence on Z. It was ascertained that these higher energy photons were not primarily bremsstrahlung produced by the stopping of Compton or pair electrons

18 E. G. Fuller and E. Hayward, *Comptes Rendus du Congrès International de Physique Nucléaire* (Dunod, Paris, 1959), p. 646.
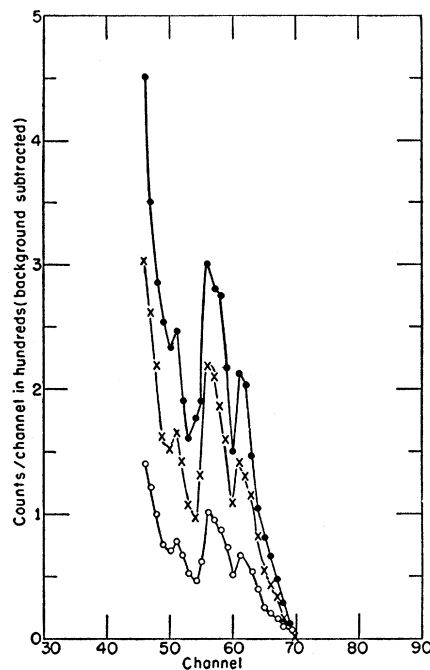
FIG. 8. Self-absorption spectra for Sn at 90°, E_p=2.05 Mev. Absorber path length=2.95 cm. Solid circles show scattered spectrum without absorber, open circles with absorber in incident beam, and crosses represent the latter spectrum corrected for electronic absorption in the absorber.

in the scatterer; the pulse-height spectrum from a lead scatterer of thickness less than $\frac{1}{5}$ the radiation length of
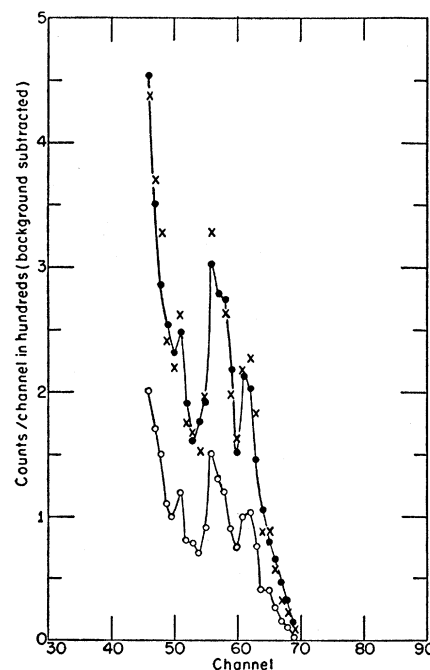
FIG. 9. Measurements corresponding to those shown in Fig. 8 but with absorber in scattered beam (in front of detector). The self-absorption effect is not evident because the scattered radiation is off resonance.

a 7-Mev electron showed the same ratio of higher energy inelastic scattering to elastic scattering as appreciably thicker targets. It seemed likely that this large inelastic scattering, which, incidentally, had been observed previously[19] in experiments at 17 Mev, was the result of several secondary or multiple electronic processes and no further attempt to determine its origin was made.

Despite the presence of a large inelastic scattering component of nonresonant origin, it was possible to extract rough values of the ratio of elastic to inelastic resonant scattering from the self-absorption data. This was done by comparing the normalized count rates for inelastic scattering with and without an absorber, normalization being accomplished through the count rates for elastic scattering with and without an absorber. The details of the calculation giving the branching ratio, $\Gamma_{\gamma 0}/\Gamma_\gamma$, in terms of measured quantities are presented in Appendix A. The branching ratios obtained in this way are subject to considerable uncertainty for two reasons. First, the electronic part of the inelastic scattering is dominant, which leads to the subtraction of two large and almost equal count rates in comparing inelastic scattering with and without an absorber. Second, the large background and the limitations of the scintillation counter combine to prevent measurement of the differential spectrum of the nuclear cascade radiation which would ensure proper counting of the photons arising from the various alternative radiative transitions. Measurement of the integrated inelastic scattering, which was necessarily adopted here, may, however, be an adequate substitute if the low-energy limit is appropriately chosen. The nature of the cascade radiation following neutron capture has been discussed by Kinsey.[20] Briefly, for nuclei with atomic weights greater than about 70, the multiplicity of gamma rays per neutron capture is 3 to 4. If the spectrum is divided into partial spectra with the "primary" spectrum defined as that emitted by the capturing state, the "secondary" spectrum as that of the second gamma ray to be emitted, and so on, then the number of effective partial spectra is approximately equal to the multiplicity. Partial spectra calculated for the customary exponential level density function and a dipole transition probability proportional to the cube of the gamma-ray energy show not much dependence on the level density in the nucleus and, in fact, there is little difference between the spectra of nuclei with few or many excited states. The spectrum departs from normal, i.e., is biased toward higher energies, only when radical departures from the usual level densities occur as in the heaviest magic elements. Largely on the basis of these considerations, the low-energy limit of the measured inelastic scattering was chosen as 3 Mev. With this lower limit the cal-

culated partial spectra indicate it is quite unlikely that more than one gamma ray from a given cascade is counted or that more than 25% of the total number of transitions are missed. This uncertainty is less than that introduced by the large nonresonant inelastic scattering which limits the accuracy of the branching ratios as shown in the last column of Table IV.

Comparison of Results

The measured differential cross sections for oxygen at 90 and 120 degrees and at $E_p = 2.05$ and $E_p = 2.40$ Mev and the known spins of the 7.12- and 6.92-Mev levels of O^{16} permit direct calculation of the lifetimes of the latter two levels. Within our accuracy, the two levels have the same mean life of $(1.0\pm0.3)\times10^{-14}$ sec which is to be compared with the values of $(1.2\pm0.3) \times10^{-14}$ sec and $(1.0\pm0.3)\times10^{-14}$ sec for the 6.92- and 7.12-Mev levels, respectively, obtained by Swann and Metzger.[12]

The energy dependence of the elastic photon scattering cross sections of medium and heavy elements has been studied by Fuller and Hayward[21] using a bremsstrahlung spectrum. For seven of the ten elements measured in both experiments, the cross sections at 7 Mev obtained from their excitation functions are consistently larger than those given in Table II by a factor varying from 2 to 5. For lead and bismuth, which have the largest cross sections measured, the agreement is good. For aluminum, which appears to have a very low cross section, their value is 30 times larger than the upper limit given here.

IV. DISCUSSION

Level Parameters

The elastic scattering cross sections and the self absorption data are related to the level parameters of the scattering nuclei in an involved manner; however, average values of the parameters can be extracted from these relationships providing the levels in the region of interest are nonoverlapping. There are two independent measurements which place an upper limit on the ratio of level width to level spacing. First, measurements of the photon intensity during "direct" runs with and without an absorber permit us to place an upper limit of 0.1 on the ratio of nuclear absorption to electronic absorption over the energy interval in question. The measured branching ratios in conjunction with the expression for the peak absorption cross section of a single level then give a ratio of level width to level spacing of less than 0.15 for all of the elements investigated. Second, self-absorption measurements with the absorber in the scattered rather than in the incident beam show no self-absorption effect (see Fig. 9), indicating that the recoil energy lost to the scattering nucleus throws the re-emitted radiation off resonance.

[19] M. B. Stearns, Phys. Rev. 87, 706 (1952).
[20] B. B. Kinsey, *Handbuch der Physik* (Springer-Verlag, Berlin, 1957), Vol. 40.

[21] E. G. Fuller and E. Hayward, Phys. Rev. 101, 692 (1956).

This implies a width to level spacing ratio of less than 0.3, since a larger value would result in an effect outside our experimental error. These limits tend to support the assumption that the levels of concern here do not overlap and that, for this reason, an analysis based on individual level properties should be valid.

We proceed now to obtain an expression connecting the quantities measured in a self-absorption experiment with certain average nuclear energy level parameters which, providing the branching ratio to the ground state is known, leads to evaluation of an average level width. In the limit of zero absorber thickness and for a thin scatterer we obtain the relation between the average level parameters and the cross section for elastic scattering averaged over the energy range of the incident photon spectrum.

The number of photons per unit energy interval scattered by an element of thickness dz at a depth z in a given scatterer may be written as

$$S(E,z)dz = N(E) \exp[-2\sigma'(E)nz]$$
$$\times \exp[-\sigma_1(E)nz]\sigma_2(E)ndz, \quad (1)$$

where $N(E)$ is the number of photons per unit energy interval incident on the scatterer, $\sigma'(E)$ is the electronic cross section, $\sigma_1(E)$ is the cross section for nuclear absorption, $\sigma_2(E)$ is the cross section for elastic scattering and n is the number of target nuclei per unit volume. In an actual experiment one measures the differential scattering cross section at a given scattering angle θ, and it is convenient to define

$$\sigma_2(E,\theta) = \sigma_2(E)W(\theta), \quad (2)$$
with
$$\int W(\theta)d\Omega = 1.$$

If now we introduce an absorber of effective thickness T into the incident photon beam, then the total number of photons elastically scattered at angle θ by a scatterer of effective thickness L that will be recorded by a counter with efficiency $\eta(E)$ is given by

$$\int_0^L C(T+z, \theta)dz$$

$$= \frac{n\Omega_s\Omega_d}{4\pi} \int_0^L \int_{\Delta E} I(E)\eta(E) \exp[-\sigma'(E)nT]$$

$$\times \exp[-2\sigma'(E)nz] \exp[-\sigma_1(E)n(T+z)]$$

$$\times \sigma_2(E,\theta)dEdz, \quad (3)$$

where Ω_d is the solid angle subtended by the detector at the scatterer, Ω_s is the solid angle subtended by the scatterer at the source and $I(E)$ is the total number of photons per unit energy interval emitted by the source.

We note that $I(E)$, $\eta(E)$, and $\sigma'(E)$ are slowly varying functions which may be taken outside the energy integral and set equal to their values at an average energy $\bar{E}$ over the incident spectral range ΔE. We may then express the quantities standing before the integrals of Eq. (3) in terms of directly measured count rates. The experimental procedure described earlier leads to the following definitions:

$$C_{ms} = [I(\bar{E})/4\pi]\Delta E\eta_m(\bar{E})\Omega_m \quad (4)$$

is the number of counts recorded by the monitor (subscript m) during a scattering measurement.

$$C_{dd} = [I'(\bar{E})/4\pi]\Delta E\eta(\bar{E})\Omega_d \exp[-\sigma'(\bar{E})nT] \quad (5)$$

is the number of counts in the elastic region of the pulse-height spectrum recorded by the detector when it is in the scatterer, i.e., "direct," position. The term containing $\sigma_1(E)$ has been omitted in Eq. (5) because the integrated nuclear absorption is too small to be observed in a simple transmission experiment.

$$C_{md} = [I'(\bar{E})/4\pi]\Delta E\eta_m(\bar{E})\Omega_m \quad (6)$$

is the number of counts recorded by the monitor when the detector is in the "direct" position. In general, the incident beam intensity in a "direct" run, $I'(\bar{E})$, is appreciably less than the intensity in a scattering run, $I(\bar{E})$. Combining (4), (5) and (6), we have

$$(C_{ms}C_{dd}/C_{md}) = [I(\bar{E})/4\pi]\Delta E\eta(\bar{E})\Omega_d$$
$$\times \exp[-\sigma'(\bar{E})nT], \quad (7)$$

and we see that the exponential term takes into account electronic absorption in the absorber and no independent information concerning the incident beam strength or detector efficiency is necessary. We may also write

$$\Omega_s = N/nLR^2, \quad (8)$$

where R is the mean distance from source to scatterer which is also equal to the mean distance from scatterer to detector and N is the total number of scattering nuclei. If further we set

$$C_{ds} = \int_0^L C(T+z, \theta)dz \quad (9)$$

as the number of counts in the elastic region of the pulse-height spectrum recorded by the detector during a scattering measurement, we find

$$C_{ds} = \frac{C_{ms}C_{dd}N}{C_{md}\Delta ELR^2} \int_0^L \exp[-2\sigma'(\bar{E})nz]$$

$$\times \int_{\Delta E} \sigma_2(E,\theta) \exp[-\sigma_1(E)n(T+z)]dEdz. \quad (10)$$

Now the cross section for excitation of a single level by photon absorption and the subsequent de-excitation from that level may be written[6]

$$\sigma_a(x,t) = \sigma_0 g(\Gamma_{\gamma 0}\Gamma_a/\Gamma^2)\psi(x,t), \quad (11)$$

where $\Gamma_{\gamma 0}$ is the partial width for transitions between the given excited level and the ground state, Γ_a is the partial width for de-excitation by mode a, Γ is the total width of the level, $\sigma_0 = 4\pi\lambda^2$ with λ the wavelength of radiation at exact resonance divided by 2π and $g = (2J_2+1)/2(2J_1+1)$ with J_2 and J_1 the spins of the excited and ground states, respectively. Further

$$\psi(x,t) = \frac{1}{2(\pi t)^{\frac{1}{2}}} \int_{-\infty}^{+\infty} \frac{\exp[-(x-y)^2/4t]}{1+y^2} dy \quad (12)$$

is the Doppler integral that follows from convoluting a Maxwell distribution of velocities along a given direction with the Breit-Wigner single level formula. Here $t = (\Delta/\Gamma)^2$ with Δ, the Doppler width, equal to $E(2kT/Mc^2)^{\frac{1}{2}}$; $x = 2(E-E_R)/\Gamma$, where E is the incident photon energy and E_R is the energy of exact resonance; $y = 2(E'-E_R)/\Gamma$, with E' the Doppler shifted energy of the incoming photon as seen by the nucleus because of its thermal motion. Hence

$$\sigma_1(x,t) = \sigma_0 g(\Gamma_{\gamma 0}/\Gamma)\psi(x,t) \quad (13)$$

is the cross section for nuclear absorption, and

$$\sigma_2(x,t,\theta) = \sigma_0 g W(\theta)(\Gamma_{\gamma 0}{}^2/\Gamma^2)\psi(x,t) \quad (14)$$

is the differential cross section for elastic scattering.

We replace the cross sections $\sigma_1(E)$ and $\sigma_2(E,\theta)$ by a number of single level resonances by writing

$$\sigma_1(E) = \sum_i \sigma_1(x_i,t_i), \quad (15)$$

$$\sigma_2(E,\theta) = \sum_j \sigma_2(x_j,t_j,\theta), \quad (16)$$

so that

$$\int_{\Delta E} \sigma_2(E,\theta) \exp[-\sigma_1(E)n(T+z)]dE$$

$$= \int_{\Delta E} \sum_j \sigma_2(x_j,t_j,\theta) \exp[-\sum_i \sigma_1(x_i,t_i)n(T+z)]dE$$

$$= \sum_k \int_{\Delta E_k} \sigma_2(x_k,t_k,\theta) \exp[-\sigma_1(x_k,t_k)n(T+z)]dE,$$

where the last integral is taken over the kth resonance. The last relation makes explicit the assumption of nonoverlapping levels since then only the absorption of level k affects the scattering by level k. This expression contains more information than we are able to extract from the experimental data and we therefore define the average cross sections $\bar{\sigma}_2(x,t,\theta)$ and $\bar{\sigma}_1(x,t)$ by setting

$$\sum_k \int_{\Delta E_k} \sigma_2(x_k,t_k,\theta) \exp[-\sigma_1(x_k,t_k)n(T+z)]dE$$

$$= \rho(\bar{E})\Delta E \int_{\text{single resonance}} \bar{\sigma}_2(x,t,\theta)$$

$$\times \exp[-\bar{\sigma}_1(x,t)n(T+z)]dE; \quad (17)$$

$\bar{\sigma}_1$ and $\bar{\sigma}_2$ are then the absorption and elastic scattering cross sections of each of the $\rho(\bar{E})\Delta E$ levels with which the averaging procedure has replaced the actual levels in the interval ΔE. According to the definition of $\bar{\sigma}_1$ and $\bar{\sigma}_2$, we have

$$\bar{\sigma}_1(x,t) = \sigma_0 g\langle(\Gamma_{\gamma 0}/\Gamma)\psi(x,t)\rangle_{\text{av}}, \quad (18)$$

and

$$\bar{\sigma}_2(x,t,\theta) = \sigma_0 g W(\theta)\langle(\Gamma_{\gamma 0}{}^2/\Gamma^2)\psi(x,t)\rangle_{\text{av}}, \quad (19)$$

and we are prevented from performing the integration over E unless we assume that the $\rho(\bar{E})\Delta E$ levels that have replaced the actual levels in ΔE have identical partial and total widths. Under this assumption

$$\bar{\sigma}_1(x,t) = \sigma_0 g(\bar{\Gamma}_{\gamma 0}/\bar{\Gamma})\bar{\psi}(x,t), \quad (20)$$

and

$$\bar{\sigma}_2(x,t,\theta) = \sigma_0 g W(\theta)(\bar{\Gamma}_{\gamma 0}{}^2/\bar{\Gamma}^2)\bar{\psi}(x,t), \quad (21)$$

and we are able to integrate numerically over E providing the branching ratio, $\bar{\Gamma}_{\gamma 0}/\bar{\Gamma}$, is known, since $\psi(x,t)$ has been tabulated[22] for $0 \leq x \leq 300$ and $0 \leq t \leq 2500$. By forming the ratio appropriate to a self-absorption experiment,

$$\left[\frac{C_{ds}C_{md}}{C_{ms}C_{dd}}\right]_{T=T} : \left[\frac{C_{ds}C_{md}}{C_{ms}C_{dd}}\right]_{T=0},$$

we eliminate $\rho(\bar{E})$ and integration then leads to a unique value of $t = (\Delta/\bar{\Gamma})^2$.

Finally, we may readily find the elastic scattering cross section averaged over the interval ΔE. If we consider only a scattering experiment with a thin scatterer, such that $T=0$ and L is small, we obtain from (10) and (17) after integrating over z

$$\frac{C_{ds}C_{md}R^2}{C_{ms}C_{dd}N} = \frac{\bar{\Gamma}\rho(\bar{E})}{2} \int_{\text{single resonance}} \bar{\sigma}_2(x,t,\theta)dx, \quad (22)$$

where the quantity on the right is the differential elastic scattering cross section averaged over ΔE, i.e., $\langle\bar{\sigma}_2(\theta)\rangle$. In applying Eq. (22) to the data a correction for absorption in the scatterer is made numerically. Inserting for $\bar{\sigma}_2(x,t,\theta)$ and integrating over x and solid angle then gives

$$\langle\bar{\sigma}\rangle = (\pi/2)\sigma_0 g[\bar{\Gamma}_{\gamma 0}{}^2/\bar{\Gamma}D(\bar{E})], \quad (23)$$

where $D(\bar{E}) = 1/\rho(\bar{E})$ is the average level spacing in ΔE and we have dropped the subscript on $\bar{\sigma}$.

For many of the elements investigated here we may in the expressions above insert $\bar{\Gamma}_\gamma$, the total radiation width, for $\bar{\Gamma}$ because the energy of the incident radiation is less than the threshold for neutron emission by those elements. In particular, three of the six elements (Cu, Ag, and Bi) for which self-absorption measurements

[22] M. E. Rose, W. Miranker, P. Leak, L. Rosenthal, and J. K. Hendrickson, Westinghouse Electric Corporation Atomic Power Division Report WAPD-SR-506, 1954 (unpublished), Vols. I and II.

were made are in this category. Sn, Hg, and Pb, the other three elements, each have at least one isotope with neutron threshold less than 6.9 Mev, but, fortunately, these are of lesser relative abundance: Sn^{119} (8.6%), Sn^{122} (4.7%); Hg^{199} (16.8%), Hg^{201} (13.2%); Pb^{207} (21% and 9% in natural lead and "Pb^{206}", respectively). Since, in addition, the cross sections in Fig. 7 exhibit no apparent dependence on neutron threshold, we shall in what follows replace $\bar{\Gamma}$ by $\bar{\Gamma}_\gamma$. Thus we use the measured branching ratios, $\bar{\Gamma}_{\gamma 0}/\bar{\Gamma}_\gamma$ in the solution of the equation for the elastic self-absorption ratio to find $\bar{\Gamma}_\gamma$ and hence also $\bar{\Gamma}_{\gamma 0}$. Equation (23) then permits evaluation of $D(\bar{E})$. The averaging procedures necessary to determine g and $D(\bar{E})$ for nuclei with nonzero ground-state spins are discussed in Appendix B.

We should note that Eq. (17) may also be solved numerically in the Doppler approximation, $t = (\Delta/\bar{\Gamma})^2 \gg 1$, without knowledge of the branching ratio, and the expression for the elastic self-absorption ratio then yields $\bar{\Gamma}_{\gamma 0}/\Delta$. Within the large experimental uncertainty attached to the measured branching ratios, the values of $\bar{\Gamma}_{\gamma 0}$ obtained from the two calculations are in agreement. It is, however, questionable that the Doppler approximation is valid for some elements and we present only the results of the calculations using the branching ratios. The numerical values of the level parameters that follow from the data of Tables I and IV are given in Table V for the six elements for which complete information is available.

Features of the Resonance Fluorescence Cross Sections

Figure 7 shows striking increases of the average elastic scattering cross sections near the closed shell regions around $Z=50$ and $N=82$ (Sn, Te, and Ba) and around $Z=82$ and $N=126$ (Pb, "Pb^{206}", and Bi). It appears from the parameters in Table V that the average level spacing, while somewhat larger around

TABLE V. Derived average level parameters.[a]

Element	J_2	$\bar{\Gamma}_{\gamma 0}/\bar{\Gamma}_\gamma$	$\bar{\Gamma}_\gamma$ ev	$\bar{\Gamma}_{\gamma 0}$ ev	D[b] kev
Cu	1/2	0.15±0.1	2.5±1.0	0.4±0.2	58±48
	3/2				29±24
	5/2				19±16
Ag	1/2	0.06±0.04	5.0±3.0	0.3±0.2	11±10
	3/2				5.4±5.0
Sn	1	0.2±0.1	0.8±0.4	0.16±0.1	1.8±1.4
Hg	1	0.07±0.03	3.0±1.5	0.2±0.1	0.94±0.62
Pb^{206}	1	0.6±0.3	0.9±0.4	0.5±0.3	6.7±4.5
Pb	1	0.6±0.3	0.6±0.3	0.36±0.15	3.4±2.2
Pb[c]	1	0.2±0.1	1.0±0.5	0.2±0.1	1.3±1.0
Bi	7/2	0.3±0.2	2.5±1.5	0.75±0.5	3.9±3.7
	9/2				3.1±2.9
	11/2				2.6±2.5

[a] All measurements at $E_p = 2.05$ Mev except as indicated.
[b] Assuming D inversely proportional to $2J_2+1$.
[c] $E_p = 2.40$ Mev.

closed shells, is less important in directly influencing the scattering cross sections in those elements than the large probability for transitions to the ground state. Indirectly, the larger value of D contributes to the increased cross sections in that there are fewer transitions to levels other than the ground state because there are fewer levels at lower energy; hence the branching ratios are large in those elements. The increased cross sections for resonance fluorescence near closed shells are to be contrasted with the decrease in the cross sections for radiative capture of fast (~ 1 Mev) neutrons by the same nuclei.[23] For the latter process the capture cross section depends only on $\langle\Gamma_\gamma/D\rangle_{av}$, while the expression for $\langle\bar{\sigma}\rangle$ depends on $\bar{\Gamma}_{\gamma 0}{}^2/\bar{\Gamma}_\gamma D(\bar{E})$. It seems likely that larger values of $\bar{\Gamma}_{\gamma 0}$ and $\bar{\Gamma}_{\gamma 0}/\bar{\Gamma}_\gamma$ are also responsible for the fact that even-even nuclei systematically tend to exhibit higher resonance fluorescence cross sections than their odd-even neighbors (see Fig. 7).

For elements with A less than 40, the levels at 7-Mev excitation are expected to be spaced so far apart that very few or none should lie in the relatively small energy interval explored here. Thus, in aluminum, there does not appear to be a level in that energy interval and the elastic scattering cross section is due solely to nuclear Thomson scattering. It is interesting that the cross sections for silicon and sulfur approach that of oxygen which is the effect of scattering from two relatively narrow levels. Above $A=90$, the cross sections rise to a peak near Sn although the odd-even elements Sb and I in the same region as the peak have much lower cross sections. Finally, there is the rise to the highest cross sections of Pb and Bi. The low value for thorium, of which a significant part is due to nuclear Thomson scattering, is probably explained by its low threshold for photofission (~ 5.5 Mev).

Comparison With Other Level Parameters

It is difficult to make any detailed comparison for particular nuclei of the quantities in Table V with the corresponding quantities obtained from neutron scattering and capture experiments. Nevertheless, there appear to be three significant differences in the level parameters of heavy elements obtained by the two methods. First, the partial radiative widths, $\bar{\Gamma}_{\gamma 0}$, in Table V are on the average larger than those from radiative capture measurements by a factor of at least 10. Indeed, the partial widths found here are comparable with and in some cases larger than the values of the total radiative widths extracted from neutron experiments on heavy elements.[24] Second, the total radiative widths, $\bar{\Gamma}_\gamma$ in Table V are consistently several times larger than would be expected from neutron data. These results

[23] D. J. Hughes and D. Sherman, Phys. Rev. 78, 632 (1950).
[24] D. J. Hughes and R. B. Schwartz, Neutron Cross Sections, Brookhaven National Laboratory Report BNL-325 (Superintendent of Documents, U. S. Government Printing Office, Washington, D. C., 1958), second edition.

combine to give branching ratios, $\bar{\Gamma}_{\gamma 0}/\bar{\Gamma}_\gamma$, which again are quite large. Finally, the average level spacing, D, is quite different from the level spacing indicated by neutron scattering; the values in Table V are roughly 100 times larger, except in Pb where our value is 100 times smaller and in Bi where the two values are comparable.

These differences are perhaps not unexpected in view of the circumstance that the resonance fluorescence measurements select just those levels having large dipole transition matrix elements with the ground state. The measured level spacing indicates that these levels occur roughly about 100 times less frequently than levels not having this property. Furthermore, in any given nucleus, spin selection rules may inhibit direct transitions to the ground state after neutron capture, which would also lessen the likelihood of observation of such levels by that reaction. Following this reasoning, it would be expected that the levels described here are not essentially different from those observed in neutron experiments in the sense that all are levels in a compound nucleus involving many particle excitations and all are capable of excitation by either photons or neutrons, subject to appropriate selection and conservation rules. It should be noted, however, that the large radiative widths and level spacings in Table V are in relatively good agreement with the modified independent particle calculation of Blatt and Weisskopf[3] of the radiation width for transitions of order l between a highly excited state a and a lower state b. This calculation has been used with the radiation widths and level spacings measured in neutron capture studies to evaluate the quantity D_0 which appears in the theory, where D_0 is the spacing of low-lying single particle levels of the same spin and parity that can combine with the ground state in the transitions considered. For a single particle in a nuclear potential well, one would expect D_0 to be of the order of 15 Mev which is quite similar to the values of D_0 calculated from the parameters of Table V but considerably less than 150 Mev found by Kinsey and Bartholomew[4] and 500 Mev obtained by Levin and Hughes.[1] The import of this situation is not clear in view of the approximate nature of the calculation, but it does indicate that the wave functions of the levels with large radiation widths and average spacing possess a single particle admixture which is greater than that of the levels observed in the neutron experiments.

ACKNOWLEDGMENTS

APPENDIX A

We obtain here an expression for the branching ratio, $\bar{\Gamma}_{\gamma 0}/\bar{\Gamma}_\gamma$, in terms of quantities measured in a self-absorption experiment.

As discussed in Sec. III, the cross section for inelastic scattering, σ_i, is made up of the contributions of inelastic nonresonant scattering, σ_{nr}, and of inelastic resonant scattering, $\bar{\sigma}_{ir}$, where $\bar{\sigma}_{ir}$ is given by

$$\bar{\sigma}_{ir} = \frac{\pi}{2}\sigma_0 g \frac{\bar{\Gamma}_{\gamma 0}}{D}\left(\frac{\bar{\Gamma}_\gamma - \bar{\Gamma}_{\gamma 0}}{\bar{\Gamma}_\gamma}\right). \tag{A1}$$

In a self-absorption experiment the nuclei in the absorber selectively absorb those photons which would excite the scatterer nuclei and this results in a decrease in the measured scattered radiation. The cross sections for nuclear absorption and scattering are, of course, not changed by the presence of an absorber, but it is convenient to describe the effect of an absorber by means of apparently changed cross sections which we indicate without average signs. Thus we write

$$\sigma_i \text{ (with absorber)} = \sigma_{ir} \text{ (with absorber)} + \sigma_{nr}, \tag{A2}$$

and

$$\sigma_i \text{ (without absorber)}$$
$$= \sigma_{ir} \text{ (without absorber)} + \sigma_{nr}. \tag{A3}$$

The quantities on the left may be considered as directly measured because the relation, $\sigma_e/C_e = \sigma_i/C_i$ provides σ_i in terms of the cross section for elastic scattering, σ_e, and the measured number of elastic and inelastic counts, C_e and C_i, respectively. This relation is valid to better than 10% because the total detection efficiency of a NaI detector for photons in the energy range from 3 to 7 Mev varies by less than that amount. We have also left σ_{nr} unaffected by the presence of an absorber in Eqs. (A2) and (A3) because our experimental procedure corrects empirically for electronic absorption in the absorber [see Eq. (5)].

If now we note that the measured attenuation in a self-absorption experiment affects both the resonant elastic and resonant inelastic effective cross sections to the same extent, then we have

$$\frac{\sigma_e \text{ (with absorber)}}{\sigma_e \text{ (without absorber)}} = \frac{\sigma_{ir} \text{ (with absorber)}}{\sigma_{ir} \text{ (without absorber)}}. \tag{A4}$$

Equations (A2), (A3), and (A4) provide the quantities σ_{ir} (with absorber), σ_{ir} (without absorber) and σ_{nr} in terms of the other directly measured quantities. From Eq. (A1) and Eq. (23) of Sec. IV, we obtain

$$\frac{\bar{\sigma}_{ir}}{\bar{\sigma}_e} = \frac{\bar{\Gamma}_\gamma - \bar{\Gamma}_{\gamma 0}}{\bar{\Gamma}_{\gamma 0}} \tag{A5}$$

from which, finally

$$\Gamma_{\gamma 0}/\Gamma_{\gamma}$$

$$=\left[1+\frac{\sigma_i \text{ (without absorber)} - \sigma_i \text{ (with absorber)}}{\sigma_e \text{ (without absorber)} - \sigma_e \text{ (with absorber)}}\right]^{-1}.$$

(A6)

APPENDIX B

In the preceding discussion we have treated the quantity $g = (2J_2+1)/2(2J_1+1)$ as known. However, J_2 is uniquely defined for a given multipolarity transition only if $J_1=0$. For $J_1 \neq 0$, J_2 can in general take on any one of several values. Since the measured cross sections represent contributions from many levels, it is reasonable to average over the various possible J_2 values, assigning to them the relative weights $2J_2+1$.[20] Similar averaging procedures are necessary to convert a measured differential cross section at a given angle into a total cross section.

The average differential elastic scattering cross section is related to the level parameters by the equation

$$\langle\sigma(\theta)\rangle = 2\pi^2\lambda^2 g(\Gamma_{\gamma 0}^2/\Gamma D)W(\theta), \qquad (B1)$$

where $W(\theta)$ is the angular distribution function normalized so that $\int W(\theta)d\Omega = 1$ and where, for simplicity, we have omitted the bars over all quantities.

In the case $J_1 \neq 0$ we must add the angular distributions $W_i(\theta)$ corresponding to transitions from the various $J_2{}^i$ states incoherently to get a resultant angular distribution. We assume that $\Gamma_{\gamma 0}^2/\Gamma$ does not depend on $J_2{}^i$, but that the level density, $\rho_i = 1/D_i$, does. This gives for the contribution to the differential cross section of levels having spin $J_2{}^i$:

$$\langle\sigma(\theta)\rangle_i = [2\pi^2\lambda^2\Gamma_{\gamma 0}^2/\Gamma]\rho_i g_i W_i(\theta) = M\rho_i g_i W_i(\theta), \quad (B2)$$

with g_i equal to $(2J_2{}^i+1)/2(2J_1+1)$. The differential cross section due to all the levels of different i is then obtained by summing all the contributions (B2):

$$\langle\sigma(\theta)\rangle = \sum_i \langle\sigma(\theta)\rangle_i = M \sum_i \rho_i g_i W_i(\theta)$$
$$= M\langle W(\theta)\rangle \sum_i \rho_i g_i, \qquad (B3)$$

where

$$\langle W(\theta)\rangle = \sum_i \rho_i g_i W_i(\theta)/\sum_i \rho_i g_i \qquad (B4)$$

is the resultant average angular distribution function normalized so that $\int\langle W(\theta)\rangle d\Omega = 1$. It follows immediately that

$$\langle\sigma\rangle = \int \langle\sigma(\theta)\rangle d\Omega = M \sum_i \rho_i g_i. \qquad (B5)$$

The relation between the total cross section and the differential cross section measured at a given angle α is then found from the three equations preceding to be

$$\langle\sigma\rangle = \langle\sigma(\alpha)\rangle \sum_i \rho_i g_i/\sum_i \rho_i g_i W_i(\alpha). \qquad (B6)$$

To determine the various $W_i(\theta)$ we make use of the fact that the angular correlation between an incident photon which excites a nucleus from state J_1 to state J_2 and the photon emitted when the nucleus de-excites to state J_1 is the same as the angular correlation between two successive transitions $J_1 \rightarrow J_2 \rightarrow J_1$.[25] The correlation coefficients are then easily calculated using the tables by Biedenharn and Rose.[26]

In the expression for the ratio of elastic scattering with and without an absorber we must, in the case $J_1 \neq 0$, insert an effective averaged g of the form

$$\langle g\rangle = \frac{1}{2(2J_1+1)}\frac{\sum_i (2J_2{}^i+1)^2}{\sum_i (2J_2{}^i+1)}. \qquad (B7)$$

To find D_i we make use of Eq. (23) and the $2J_2{}^i+1$ level density dependence, which finally leads to

$$D_i = \left[\frac{\pi^2\lambda^2\Gamma_{\gamma 0}^2}{(2J_1+1)(2J_2{}^i+1)\Gamma\langle\sigma\rangle}\right]\sum_i (2J_2{}^i+1)^2. \qquad (B8)$$

[25] D. R. Hamilton, Phys. Rev. 58, 122 (1940).
[26] K. Siegbahn, Beta- and Gamma-Ray Spectroscopy (North Holland Publishing Company, Amsterdam, 1955), Chap. XIX and Appendix V.